Mon. Not. R. Astron. Soc. **389,** 792–798 (2008) doi:10.1111/j.1365-2966.2008.13576.x

A young, dusty, compact radio source within a Lyα halo

F. Eugenio Barrio,[1⋆] Matt J. Jarvis,[1,2⋆] Steve Rawlings,[1] Amanda Bauer,[3,4] Steve Croft,[5,6,7] Gary J. Hill,[3] Arturo Manchado,[8] Ross J. McLure,[9] Daniel J. B. Smith[1,10] and Thomas A. Targett[9]

[1]*Astrophysics, Department of Physics, Keble Road, Oxford OX1 3RH*
[2]*Centre for Astrophysics Research, Science & Technology Research Institute, University of Hertfordshire, Hatfield AL10 9AB*
[3]*University of Texas at Austin, Austin, TX 78712, USA*
[4]*Gemini Observatory, Southern Operations Centre c/o AURA, Casilla 603, La Serena, Chile*
[5]*Institute of Geophysics and Planetary Physics, Lawrence Livermore National Laboratory L-413, 7000 East Ave, Livermore, CA 94550, USA*
[6]*UC Berkeley, 601 Campbell Hall 3411, Berkeley, CA 94720, USA*
[7]*UC Merced, P.O. Box 2039, Merced, CA 95344, USA*
[8]*Instituto de Astrofísica de Canarias, c / Vía Láctea s/n, 38205 La Laguna, Tenerife, España*
[9]*Institute for Astronomy, University of Edinburgh, Royal Observatory, Blackford Hill, Edinburgh EH9 3HJ*
[10]*Astrophysics Research Institute, Liverpool John Moores University, Egerton Wharf, Birkenhead CH41 1LD*

Accepted 2008 June 12. Received 2008 June 9; in original form 2007 June 21

ABSTRACT

We report here on the discovery of a red quasar, J004929.4+351025.7 at a redshift of $z = 2.48$, situated within a large Lyα emission-line halo. The radio spectral energy distribution implies that the radio jets were triggered $<10^4$ yr prior to the time at which the object is observed, suggesting that the jet triggering of the active galactic nucleus is recent. The loosely biconical structure of the emission-line halo suggests that it is ionized by photons emitted by the central quasar nucleus and that the central nucleus is obscured by a dusty torus with $A_V \sim 3.0$. The large spatial extent of the Lyα halo relative to the radio emission means this could only have occurred if the radio jets emerged from an already established highly accreting black hole. This suggests that the radio jet triggering is delayed with respect to the onset of accretion activity on to the central supermassive black hole.

Key words: galaxies: active – galaxies: haloes – galaxies: high-redshift – quasars: individual: J004929+351025.

1 INTRODUCTION

Most quasars exhibit a blue optical and ultraviolet continuum, broad emission lines and narrow forbidden emission lines of highly ionized elements (e.g. Schneider et al. 2003). However, there is also a population of reddened quasars predicted by the unification schemes (Urry & Padovani 1995), and which have been known for a number of years (e.g. Webster et al. 1995). The origin of red quasars and their fraction relative to normal quasars is still subject of debate: we still do not know the fraction that are intrinsically red, e.g. in radio-loud quasars the synchrotron tail can extend into the near-infrared and optical wavebands (Whiting, Webster & Francis 2001), or the fraction that are reddened by dust (e.g. Richards et al. 2003). For the dusty quasars, it is not clear if the dust is typically situated in a dusty torus around the central quasar nucleus (e.g. Antonucci 1993), or whether it is distributed more widely throughout the host galaxy (e.g. Martínez-Sansigre et al. 2006).

⋆Email: febm@astro.ox.ac.uk (FEB); m.j.jarvis@herts.ac.uk (MJJ)

Determining the fraction of very red quasars (red, reddened or both) in the total population is essential for a precise determination of the quasar luminosity function (LF) and also for understanding the evolution of quasars and the nature of the quasar–galaxy connection. If a large fraction is eliminated from optical surveys by simple dust reddening then the relative comoving space density of such objects may be much higher and would have a much more profound effect on the evolution of massive galaxies.

Historically optical surveys, relying on the ultraviolet excess and power-law shape of the typical (i.e. blue) quasar spectrum, have failed to discover this red population, principally due to the fact that the blue excess is not present in reddened quasars (Richards et al. 2004). Unsurprisingly, recent radio and infrared surveys have shown a better promise in finding red quasars over all redshifts (Glikman et al. 2007). Although previous large area attempts have suffered from incompleteness, this is still the most promising approach.

Many powerful, high-redshift radio-loud active galactic nuclei (AGN) are now known to be surrounded by large-scale, highly luminous, Lyα emission-line haloes (Chambers, Miley & van Breugel 1988; Villar-Martín et al. 2002; Reuland et al. 2003). Similar Lyα

emission haloes have also been found around a radio-quiet quasar (Weidinger et al. 2005) and submillimetre galaxies (Steidel et al. 2000; Bower et al. 2004; Chapman et al. 2004; Geach et al. 2005). This suggests that giant Lyα haloes may be associated with the onset of quasar and/or starburst activity (see also Haiman & Rees 2001; Ohyama et al. 2003; Wilman et al. 2005). However, the recent discovery of a number of large diffuse Lyα haloes around seemingly quiescent galaxies (Nilsson et al. 2006; Saito et al. 2007; Smith & Jarvis 2007) suggests a model in which the origin of some Lyα haloes is cold gas accreting on to the dark matter halo of a massive galaxy (Fardal et al. 2001; Dijkstra et al. 2006). There may therefore be several mechanisms responsible for giant Lyα haloes. However, most of the large >50 kpc haloes discovered so far seem to surround massive galaxies, thus the large haloes may be a product or a requisite ingredient in the formation of massive galaxies at high redshift, regardless of the mechanism behind their ionization.

In this paper we report the discovery of a reddened quasar that conforms to the idea that red, young, radio quasars at $z \sim 2.5$ might pick out dusty, possibly star-forming massive galaxies within giant Lyα haloes. In Section 2 we present the photometric and spectroscopic data and in Section 3 we discuss the properties of this object. In Section 4 we make some concluding remarks concerning the implications of this object for jet triggering in AGN. We assume throughout that $H_0 = 70\,\mathrm{km\,s^{-1}\,Mpc^{-1}}$, $\Omega_\mathrm{M} = 0.3$ and $\Omega_\Lambda = 0.7$. All quoted magnitudes are in the Vega system.

2 DATA AND OBSERVATIONS

2.1 Quasar discovery

J004929.4+351025.7 (hereafter J0049+3510) was initially found by cross-matching the 325-MHz Westerbork Northern Sky Survey (WENSS; Rengelink et al. 1997) and the 1.4-GHz Northern VLA Sky Survey (NVSS; Condon et al. 1998) radio source catalogues as part of our survey for $z > 6$ quasars (Jarvis et al. 2004). It has a 325-MHz flux density of $S_{325\,\mathrm{MHz}} = 101 \pm 18$ mJy and a 1.4-GHz flux density of 122.0 ± 3.7 mJy, giving an inverted radio spectrum between 325 MHz and 1.4 GHz, $\alpha^{1.4\,\mathrm{GHz}}_{325\,\mathrm{MHz}} = -0.134$. As inspection of the Digitized Sky Survey showed no optical counterpart at the radio position, it was marked for follow up in the optical and near-infrared wavebands as a candidate $z > 6$ quasar.

2.2 Radio data

A search in the literature showed counterparts for J0049+3510 in the GB6 4.85 GHz survey (Gregory et al. 1996) but no counterparts in the 6C 151 MHz survey (Hales et al. 1993), nor the VLSS 74 MHz survey (Cohen et al. 2007). The source position is not covered by the FIRST (Faint Images of the Radio Sky at Twenty-cm) survey (Becker, White & Helfand 1995).

Archive observations from the Very Large Array (VLA), in A array, *X* band (8.0–8.8 GHz), were recovered and a map made from the data available. This revealed a compact radio source (unresolved at 0.3 arcsec resolution) with a flux density $S_{8\,\mathrm{GHz}} = 33.4 \pm 1.4$ mJy (see Table 1). The radio spectrum of J0049+3510 is shown in Fig. 1, and it is apparent that the spectral energy distribution (SED) is peaked around 1.2 GHz. Given the compact nature and the peak of the SED at 1.2 GHz we classify this quasar as a Giga-Hertz Peaked Spectrum (GPS; O'Dea 1998) source.

Table 1. Summary of radio properties of J0049+3510. The quoted limits are 5σ.

Survey	Frequency (GHz)	Flux density (mJy)
VLA	8.4	33.4 ± 1.4
GB6	4.85	67 ± 9
NVSS	1.4	122.0 ± 3.7
WENSS	0.325	101 ± 18
6C	0.151	<400
VLSS	0.074	<500

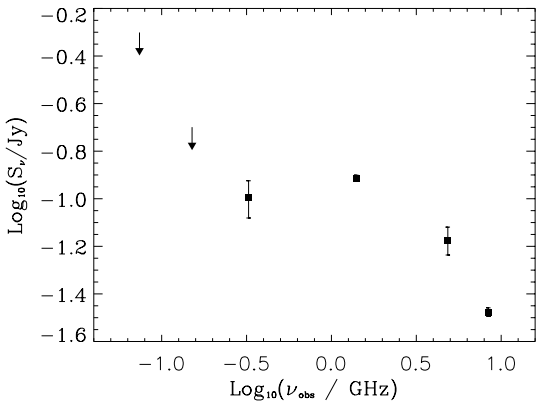

Figure 1. Observed-frame radio SED for J0049+3510. The peak of the SED is shown to be around 1.2 GHz (4.2 GHz in the rest frame for $z \sim 2.5$), corresponding to a source age of $\sim 10^3$ yr (see O'Dea 1998).

2.3 Optical and near-infrared imaging

The quasar was subsequently observed at Harlan J. Smith Telescope (HJST) at McDonald Observatory for 150 s in the *R* band. The data were bias-subtracted, flat-fielded and combined with standard IRAF packages. For flux calibration we used standard stars observed on the same night. Aperture photometry was performed using the IRAF APPHOT package with a 2-arcsec-diameter aperture. No identification was found at the position of the radio source, implying that our source was fainter than $R \simeq 23.9$ mag at the 3σ level.

Following our search method, we targeted it with near-infrared *K*-band imaging on the United Kingdom Infrared Telescope (UKIRT) with good seeing conditions (<0.6 arcsec). The UKIRT imaging was carried out with the UKIRT Fast Track Imager (UFTI) using the standard nine-point jitter pattern and reduced using ORACDR pipeline, which subtracts the dark current and flat-fields the data with a median sky-flat constructed from the individual science frames. These observations showed an unresolved source within 0.5 arcsec of the radio position with $K = 17.62 \pm 0.07$ (Fig. 2).

J0049+3510 was then targeted in *J*- and *H* bands, again, with the UKIRT-UFTI using the same strategy as for the *K*-band observations, which showed that it was also identified in the *H* band with $H = 18.69 \pm 0.15$, however, the *J*-band observations were carried out in poor conditions and an accurate *J*-band magnitude could not be obtained.

Subsequent deep optical *I*-band imaging on the William Herschel Telescope (WHT) produced blank fields with a limit of $I > 24.5$ (3σ). Deep *J*-band observations were also carried out with the Long-slit Intermediate Resolution Infrared Spectrograph (LIRIS) on the WHT, these observations showed a point source with

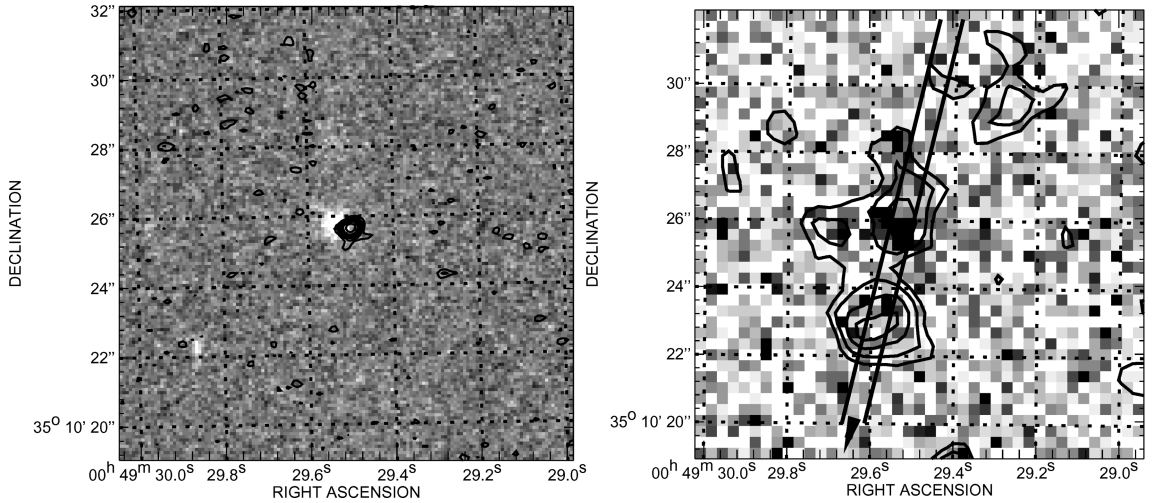

Figure 2. Left: *K*-band image (grey-scale) overlayed with the radio 8 GHz (contours) showing the compact radio source matching the unresolved near-infrared object within the astrometric uncertainty of the *K*-band image. The radio contours are -2σ and $2^{n/2}\sigma$, where $n = 2, 3, 4, \ldots, 14$ with $\sigma = 282$ μJy. Right: the *K*-band image (grey-scale) is overlayed with the optical *g* band (contours) showing diffuse blue emission near to our source and a detection of the quasar itself, which we called the south and central blobs, respectively. There is also tentative evidence for further Lyα emission to the north-west of the central source. However, this is at a much lower level than the central and southern components. There are no cospatial identifications for either the southern and northern components down to $K = 19$ (3σ). We have also added the position of the long slit used in the WHT-ISIS spectroscopy.

Table 2. Summary of optical and near-infrared imaging observations and photometry of J0049+3510. Quoted limits are 3σ. J0049+3510 is a point source in the *J*-, *H*- and *K*-band images.

Date	Telescope and instrument	Filter	Exposure (s)	Seeing (arcsec)	Aperture (arcsec)	Magnitude (Vega)
2004 December 13	INT-WFC	*g*	1800	1.1	10	19.56 ± 0.15
2003 August 28	HJST-IGI	*R*	150	1.2	2	>23.9
2003 September 22	WHT-PFIP	*I*	1200	1.2	2	>24.5
2004 November 4	WHT-LIRIS	*J*	3000	0.6	2	21.06 ± 0.20
2003 September 26	UKIRT-UFTI	*H*	540	0.7	2	18.69 ± 0.15
2003 September 15	UKIRT-UFTI	*K*	540	0.5	2	17.62 ± 0.07

$J = 21.06 \pm 0.20$ in 0.6 arcsec seeing. A summary of the optical and near-infrared photometry data is presented in Table 2.

At this stage J0049+3510 was considered a good candidate for a $z \geq 6$ quasar as the optical and near-infrared SED suggested the presence of a steep spectral break between the near-infrared and optical bands. This would correspond to the Gunn–Peterson trough, with the Lyα line redshifted between the *I*- and *J* bands. We therefore sought spectroscopy in order to determine the redshift and nature of this source.

2.4 Optical and near-infrared spectroscopy

Near-Infrared spectroscopy observations were performed with the UKIRT Imaging Spectrometer (UIST) using the standard 'ABBA' nodding sequence (with a nod of 12 arcsec) on the night of 2004 September 16. The total exposure time was 160 min and the data were reduced with ORACDR. The spectrum was extracted over 1.2 arcsec (the pixel scale is 0.12 arcsec pixel^{-1}) with the IRAF APEXTRACT packages. We identified a broad emission line at 2.292 μm, first identified, in view of the optical and near-infrared SED, as the Mg II λ2799 line redshifted to $z = 7.2$. No other obvious lines were identified in the *HK* spectrum, but continuum was present throughout the wavelength range. Fig. 3 shows the extracted one-dimensional near-infrared spectrum of the quasar. The spectrum also shows tentative evidence for a second emission line at 1.74 μm which we later confirmed to be the [O III] doublet at a redshift of $z \sim 2.48$, thus suggesting that the bright emission line may be Hα.

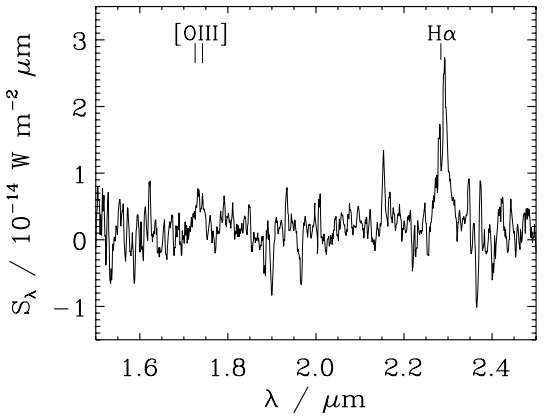

Figure 3. Near-infrared *HK* spectrum of quasar J0049+3510. The spectrum has been smoothed using a 0.003 μm FWHM Gaussian, with the broad Hα line at 2.292 μm, and a very weak [O III] doublet confirming the redshift of this source as $z = 2.48$.

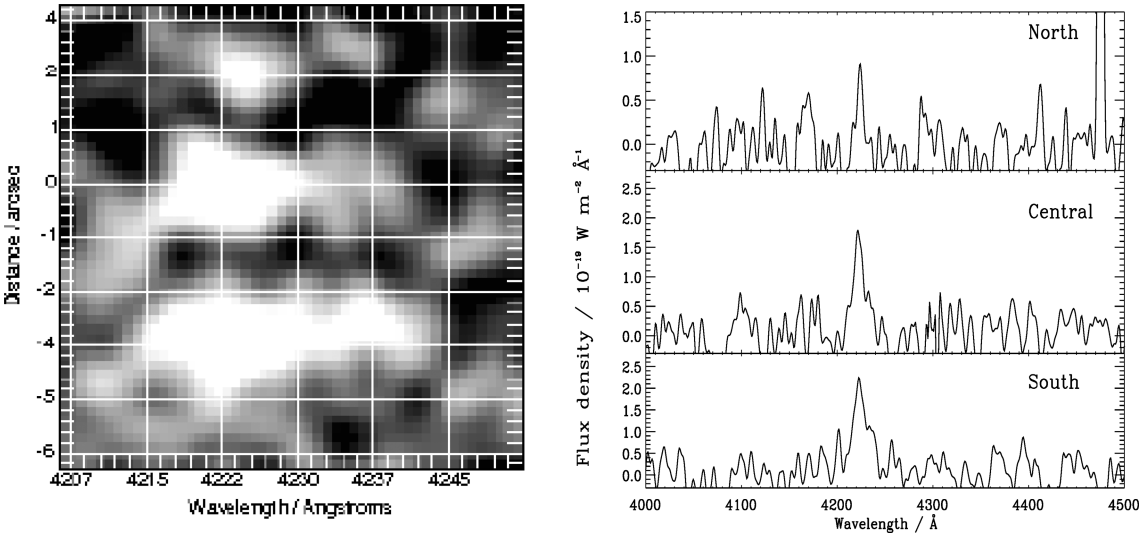

Figure 4. The left-hand panel is the two-dimensional optical spectrum centred one the position of the host galaxy and smoothed over 3 pixel showing two clear and a third tentative spatially distinct Lyα blobs at the same wavelength. The right-hand panel shows spectra of the three blobs of emission: the central spectrum is from the central region cospatial with the *K*-band identification; the top and bottom spectrum are from the northern and southern blob shown in Fig. 2. An emission line is detected at 4222 Å and identified with Lyα at $z = 2.47$ in all three blobs.

If the redshift were indeed $z = 2.48$ or 7.2, then we should be able to detect the Lyα line with optical spectroscopy.

Optical spectroscopy was carried out with the Gemini Multi-Object Spectrograph (GMOS) on Gemini-North. We used a 0.75-arcsec-long slit with position angle (PA) of 78° with a nodding of 10 arcsec. We selected the G150 grating centred at 750 nm for a total exposure time of 1200 s. The data were reduced with IRAF and a spectrum was wavelength-, flux calibrated and extracted over 1.5 arcsec (the spatial scale was 0.145 arcsec pixel^{-1}) with our own IDL routines. The spectrum showed no lines but a very faint continuum roughly between 4800 and 8000 Å. The seeing, measured as the full width at half-maximum (FWHM) of a Gaussian fit to the spatial profile of an unresolved object on the slit, was 1.3 arcsec.

2.5 The Lyα halo

The quasar was observed using the Sloan–Gunn *g* (≈420–550 nm) filter used with the Isaac Newton Telescope Wide Field Camera (INT-WFC) for 1800 s during the night of 2003 December 13. The image showed extended diffuse structure to the south of the quasar position in addition to some emission cospatial with the unresolved *K*-band identification which we take to be dominated by line emission; we refer to these as the south and central blobs, respectively. Fig. 2 shows the *K*-band image overlayed with the radio contours and also with the contours representing the *g*-band image. There is also tentative evidence for further Lyα emission towards the north of the source, which is much fainter than the central and southern components. However, we believe it to be part of the halo, although deeper observations are needed to confirm this.

Subsequent WHT-ISIS (Intermediate dispersion Spectrograph and Imaging System) spectroscopy on 2004 December 9 targeted the brightest two (central and south) blobs using a 2-arcsec slit with PA of 170° east of north, with a total exposure time of 40 min. We used the R300B grating, giving a spectral resolution of ∼9 Å. The ISIS spectra were reduced with IRAF, wavelength calibrated with a CuAr+CuNe arc and flux calibrated using observations of the SP1942+261 standard star. The one-dimensional spectrum was extracted with the IRAF APEXTRACT task for several different apertures.

Fig. 4 shows the two-dimensional spectrum, where three separate emissions lines can be identified, associated with the three blobs present in the *g*-band image; together with one-dimensional spectra extracted from each blob. We find an emission line at 4222 Å in the central and southern blobs, which we identify as Lyα, corresponding to a redshift of $z = 2.47$. No other lines (e.g. C IV, He II, C III etc.) could be found associated with either blob. The combined flux from all of the Lyα blobs, after correcting for the aperture and the edge of the filter, can account for ∼90 per cent of the flux seen in the *g*-band image. Furthermore, the spectrum taken with GMOS-N, where only the central blob is positioned on the slit, shows some faint continuum of the order $g \sim 22$; which corresponds to ∼30 per cent of the contribution of the central blob.

This result is consistent with the *K*-band emission line being Hα at $z = 2.49$; and not Mg II as it was first thought. With this established, the tentative line in the *HK* spectrum is now confirmed as the [O III] λ4959/5007 doublet at ∼1.74 μm (Fig. 3). We, therefore, use the redshift determined form the [O III] λ5007 line (i.e. $z = 2.48$), as the best estimate for the redshift of our source. We chose not to trust the redshift from the Lyα line as this could be affected by absorption and thus its position is more uncertain, while the Hα line is likely to be contaminated with other emission lines, e.g. [N II]. The emission-line properties are summarized in Table 3.

The southern blob extends to ∼4 arcsec (∼33 kpc) from the central *K*-band identification, with the overall extent of the Lyα emission, including the northern component, spanning ∼10 arcsec (∼83 kpc), suggesting this object is embedded in a very extended Lyα halo. The deconvolved velocity widths of the Lyα lines extracted over the central and southern blob are very similar, with FWHM of 1290 ± 220 and 1550 ± 280 km s^{-1} (see Table 3). However, it is clear from Fig. 4 that there is evidence for a broader wing redward of the main Lyα emission compared to the blue side, at least in the southern component and at lower signal-to-noise ratio, possibly due to dust obscuration associated with the host galaxy extinguishing the Lyα line, in the central component. Broad red

Table 3. Results (observed values) from the optical and near-infrared spectroscopy of J0049+3510. The signal-to-noise ratio on the [O III] doublet was too low to allow measurement of the linewidth.

Line	λ_{Obs} (Å)	FWHM (km s^{-1})	Line flux (10^{-18} W m^{-2})
Hα_{6563}	22 920	3300 ± 500	1.9 ± 0.6
[O III]$_{4959/5007}$	17 340, 17 423	–	0.3 ± 0.2
Lyα (north)	4 224	<650	0.64 ± 0.26
Lyα (central)	4 222	1290 ± 220	2.4 ± 0.2
Lyα (south)	4 222	1550 ± 280	3.4 ± 0.5

wings are indicative of inflows/outflows and have been seen in superwind galaxies (e.g. Ajiki et al. 2002; Dawson et al. 2002; Saito et al. 2007). Alternatively, such a profile could also indicate the presence of a neutral hydrogen absorbing screen similar to those seen around radio galaxies of small projected linear size (e.g. van Ojik et al. 1997; Jarvis et al. 2003; Wilman et al. 2004; Binette et al. 2006). Our near-infrared spectroscopy does not have the requisite signal-to-noise ratio with which to determine the shape of the Hα line accurately. However, the fact that we see very little sign of a broadened red component in Hα leads us to suggest that the broadened red wing component, when compared to the blue side, is due to associated absorption in the blue wing of the Lyα emission.

To summarize, J004929.4+351025.7 is a radio-loud GPS source at $z = 2.48$, reasonably bright in J, H and K but invisible in both I and R down to 3σ limiting magnitudes of $R = 23.9$ mag and $I = 24.5$ mag. It has a broad Hα emission line with a very weak [O III], and it lies within 83 kpc Lyα emitting halo.

3 DISCUSSION

3.1 Origin of the Lyα halo

The radio SED of J0049+3510 (Fig. 1) shows that it is a powerful ($L_{1.4} = 7.5 \times 10^{25}$ W Hz^{-1} sr^{-1}) GPS radio source with a rest-frame peak at $\nu \sim 4.2$ GHz. Using equation (1) of O'Dea (1998) to estimate the electron lifetime of a typical GPS source we find that J0049+3510 is probably a very young radio source, viewed $<10^4$ yr after the jet-triggering event. We can also use the strong anticorrelation between the turnover frequency and the projected linear size of the source (e.g. Fanti et al. 1990) to estimate the linear size of the radio emission in J0049+3510. Using equation (4) in O'Dea (1998), for a rest-frame turnover frequency of 4.2 GHz, we find that the projected linear size would be ∼100 pc, which is consistent with jet hotspots advancing at $\sim 0.25c$ (as it has been measured in compact symmetric radio sources; Owsianik & Conway 1998) for $\sim 10^3$ yr. The inferred limit on the size is also consistent (at $z = 2.48$) with the <0.3 arcsec limiting spatial resolution of the 8.4 GHz radio observations.

If we were to consider a model in which accretion activity, and hence the optical quasar nucleus, was triggered at the same time as the radio jet, then the ionizing photons could have reached no further than $\sim(1/0.25) \times 0.3 \simeq 1$ arcsec from the nucleus and, as such, the quasar nucleus would have not be able to ionize the Lyα halo that we observe. Thus, if we expect the Lyα halo to be ionized by the central AGN, a longer living source of ionizing photons (e.g. a pre-existing accreting supermassive black hole and/or a starburst) would be required to explain the presence of Lyα emission ∼40 kpc from the nucleus. Indeed, it would take a minimum of $\sim 10^5$ yr for the photons to reach the furthermost parts of the Lyα halo. This is shorter than the expected duty cycle of a typical AGN lifetime (e.g. Martini & Schneider 2003), thus the Lyα halo could easily be photoionized by an obscured quasar, in place before the current jet activity was triggered.

3.2 Estimating the extinction

In order to investigate the reddening of the optical and near-infrared SED, we have used a simple χ^2-fitting technique to estimate the amount of extinction. We used the Sloan Digital Sky Survey (SDSS) composite quasar template (Vanden Berk et al. 2001) combined with the AGN SED from Elvis et al. (1994). To this, we applied extinction corrections for three different types of dust [Milky Way (MW), Large Magellanic Cloud (LMC) and Small Magellanic Cloud (SMC)] as in Pei (1992). We have neglected any contribution from a host galaxy principally because any such component would peak in the observed-frame SED around J band, where the emission is spatially unresolved, and secondly the host would have to be unreasonably massive ($\gtrsim 10^{12}$ M$_\odot$, corresponding to a $\gtrsim 6 L_*$ elliptical after accounting for passive evolution) to contribute even at the ∼10 per cent level. Furthermore, the K–z relation for a typical radio galaxy at $z = 2.48$ predicts a K magnitude of $K = 19.1 \pm 0.5$ (Jarvis et al. 2001a; Willott et al. 2003), ∼1.5 mag fainter than our source.

For the fitting we used our three near-infrared photometry points plus the I-band non-detection, which was included, following Martínez-Sansigre et al. (2006), by assigning a flux density and an error both equal to half the flux density limit (so $S_I = \sigma_I = 1.5\sigma_{obs}$). The best fits for the quasar extinction are shown in Fig. 5. They are almost independent of dust type and yield values for the rest-frame extinction of $A_V \sim 3$. The marginalized probability for the extinction parameter for the three different types of dust is $A_V = 2.93^{+0.18}_{-0.24}$ for MW and LMC and $A_V = 2.76^{+0.16}_{-0.24}$ for SMC.

The Lyα/Hα line ratio might give extra information on extinction on this object. However, as discussed in Eales & Rawlings (1993) it is not easy to obtain a reliable intrinsic extinction value because of the effects of resonant scattering of Lyα. Therefore, we will only use this line ratio as an independent verification of our fitting results. The line ratio measured from the central blob is 1.8; similar to those found in high-redshift radio galaxies (HzRG) by Eales & Rawlings (1993). Moreover, if we assume an intrinsic Lyα/H$\alpha = 8$ line ratio and apply an extinction of $A_V = 3$ with a MW-type dust, the Lyα/Hα line ratio we should observe is 1.9, indicating that our fitting suggests a similar extinction to the optical continuum of the quasar and the narrow emission lines. We note that this level of reddening could be due to the edge of an obscuring torus, or could be due to dust in the host galaxy, although the latter is preferred as the narrow lines too appear to be reddened.

It is also plausible that the large diffuse line emission could be caused by gas cooling on to the dark matter halo of the galaxy (e.g. Fardal et al. 2001; Dijkstra et al. 2006; Nilsson et al. 2006; Smith & Jarvis 2007; Smith et al. 2008). However, the distribution of the ionized gas suggests a loosely biconical ionization front, as would be expected from a central AGN, with an obscuring torus where the ionizing photons can only escape through the opening angle of the dusty torus. This biconical structure is seen in other radio galaxies, and most convincingly in Cygnus A (Tadhunter et al. 2003). This spatial distribution could also, in principle, be caused by a large halo of absorbing gas around the galaxy as seen in many radio galaxies with small angular sizes (e.g. van Ojik et al. 1997; Jarvis et al. 2001b, 2003; Wilman et al. 2004). However, evidence

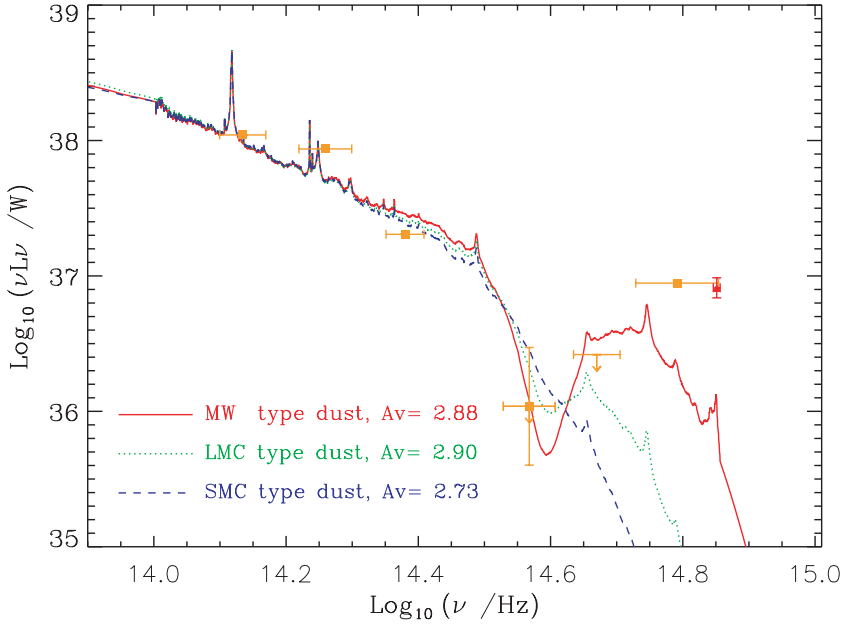

Figure 5. Near-infrared and optical SED of J0049+3510. The *KHJIR* photometric data points, and *g*-band extended emission detection (filled orange squares) suggest a reddened quasar (*I*- and *R*-band data points are 1.5σ limits). We also show the Lyα line observed on the edge of the *g* band in spectroscopy (filled red triangle). We also plot the best-fitting composite quasar spectra for different dust types (as different line styles and colours as labelled) yielding best-fitting extinctions of $A_V \approx 3$ in all cases.

suggests that such haloes may be roughly spherical in nature (Jarvis et al. 2003), and thus do not have a preferred orientation, although such gas may account for the observed broader redward component in the Lyα emission-line profile. Furthermore, there is no evidence of any other extended emission around the central source apart from in the biconical direction shown in Fig. 2.

4 CONCLUSIONS

During our search for $z > 6$ radio-loud quasars we have discovered an obscured quasar at $z = 2.48$ embedded in a large Lyα halo. The ionizing source of the large-scale Lyα halo is most likely to be the central AGN, with a dusty torus or a dusty galaxy obscuring the AGN along our line-of-sight. The dusty torus would also explain the structure of the Lyα emission-line halo, with the ionizing photons essentially being forced into a biconical distribution according to the opening angle of the torus.

Using the peak of the radio SED to estimate the age of the radio jet, we find that the radio source has been active for $\sim 10^3$ yr. assuming a jet speed of $\sim 0.25c$. This implies that the accretion activity must have started prior to the radio jet triggering event, suggesting that the triggering mechanism for the optical quasar is different, or at least not coincident in time with, the triggering of the radio jet.

Further work on J0049+3510, including integral field spectroscopy, will allow us to map the emission-line profiles across the halo and examine the nature of the ionized gas. Higher resolution radio observations would also allow us to test whether the ionizing photons are being emitted in the same direction as the young radio jet.

Completion of the follow-up for the rest of the *'red'* candidates quasars will quantify how common these type of sources are, and hopefully find some genuine $z \gtrsim 6.5$ radio-loud quasars.

ACKNOWLEDGMENTS

FEB was funded by SISCO research training network part of European Commission's 5th Framework Improving Human Potential programme. MJJ is supported by a Research Council UK fellowship. The work of SC was performed under the auspices of the US Department of Energy by the University of California, Lawrence Livermore National Laboratory under contract No. W-7405-ENG-48. SC acknowledges support for radio galaxy studies at UC Merced, including the work reported here, with the *Hubble Space Telescope* and *Spitzer Space Telescope* via NASA grants *HST* #10127, *SST* #1264353, *SST* #1265551 and *SST* #1279182. AM acknowledges support from grant *AYA 2004-3136* from the Spanish Ministerio de Educación y Ciencia. The UKIRT is operated by the Joint Astronomy Centre on behalf of the Science and Technology Facilities Council of the UK, some of the data reported here were obtained as part of the UKIRT Service Programme. The WHT and the INT are operated on the island of La Palma by the Isaac Newton Group in the Spanish Observatorio del Roque de los Muchachos of the Instituto de Astrofsica de Canarias. The Digitized Sky Surveys were produced at the Space Telescope Science Institute under US Government grant NAG W-2166. The images of these surveys are based on photographic data obtained using the Oschin Schmidt Telescope on Palomar Mountain and the UK Schmidt Telescope. The plates were processed into the present compressed digital form with the permission of these institutions. Based on observations obtained at the Gemini Observatory, which is operated by the Association of Universities for Research in Astronomy, Inc., under a cooperative agreement with the NSF on behalf of the Gemini partnership: the National Science Foundation (USA), the Science and Technology Facilities Council (UK), the National Research Council (Canada), CONICYT (Chile), the Australian Research Council (Australia), Ministrio da Cincia e Tecnologia (Brazil) and SECYT (Argentina).

REFERENCES

Ajiki M. et al., 2002, ApJ, 576, L25
Antonucci R., 1993, ARA&A, 31, 473
Becker R. H., White R. L., Helfand D. J., 1995, ApJ, 450, 559
Binette L., Wilman R. J., Villar-Martín M., Fosbury R. A. E., Jarvis M. J., Röttgering H. J. A., 2006, A&A, 459, 31
Bower R. G. et al., 2004, MNRAS, 351, 63
Chambers K. C., Miley G. K., van Breugel W. J. M., 1988, ApJ, 327, L47
Chapman S. C., Scott D., Windhorst R. A., Frayer D. T., Borys C., Lewis G. F., Ivison R. J., 2004, ApJ, 606, 85
Cohen A. S., Lane W. M., Cotton W. D., Kassim N. E., Lazio T. J. W., Perley R. A., Condon J. J., Erickson W. C., 2007, AJ, 134, 1245
Condon J. J., Cotton W. D., Greisen E. W., Yin Q. F., Perley R. A., Taylor G. B., Broderick J. J., 1998, AJ, 115, 1693
Dawson S., Spinrad H., Stern D., Dey A., van Breugel W., de Vries W., Reuland M., 2002, ApJ, 570, 92
Dijkstra M., Haiman Z., Spaans M., 2006, ApJ, 649, 14
Dunlop J. S., Peacock J. A., 1990, MNRAS, 247, 19
Eales S. A., Rawlings S., 1993, ApJ, 411, 67
Eales S. A., Rawlings S., 1996, ApJ, 460, 68
Elvis M. et al., 1994, ApJS, 95, 1
Fanti R., Fanti C., Schilizzi R. T., Spencer R. E., Nan R., Parma P., van Breugel W. J. M., Venturi T., 1990, A&A, 231, 333
Fardal M. A., Katz N., Gardner J. P., Hernquist L., Weinberg D. H., Davé R., 2001, ApJ, 562, 605
Geach J. E. et al., 2005, MNRAS, 363, 1398
Glikman E., Helfand D. J., White R. L., Becker R. H., Gregg M. D., Lacy M., 2007, ApJ, 667, 673
Gregory P. C., Scott W. K., Douglas K., Condon J. J., 1996, ApJS, 103, 427
Gunn J. E., Peterson B. A., 1965, ApJ, 142, 1633
Haiman Z., Rees M. J., 2001, ApJ, 556, 87
Hales S. E. G., Masson C. R., Warner P. J., Baldwin J. E., Green D. A., 1993, MNRAS, 262, 1057
Jarvis M. J., Rawlings S., Eales S., Blundell K. M., Willott C. J., 2001a, in Márquez I., Masegosa J., Del Olmo A., Lara L., García E., Molina J., eds, Proceedings of an International Workshop, QSO Hosts and Their Environments. Kluwer, Dordrecht, p. 333
Jarvis M. J. et al., 2001b, MNRAS, 326, 1563
Jarvis M. J., Wilman R. J., Röttgering H. J. A., Binette L., 2003, MNRAS, 338, 263
Jarvis M., Rawlings S., Barrio F., Hill G., Bauer A., Croft S., 2004, in Richards G. T., Hall P. B., eds, ASP Conf. Ser. Vol. 311, AGN Physics with the Sloan Digital Sky Survey. Astron. Soc. Pac., San Francisco, p. 361
Martínez-Sansigre A., Rawlings S., Lacy M., Fadda D., Jarvis M. J., Marleau F. R., Simpson C., Willott C. J., 2006, MNRAS, 370, 1479
Martini P., Schneider D. P., 2003, ApJ, 597, L109
Nilsson K. K., Fynbo J. P. U., Møller P., Sommer-Larsen J., Ledoux C., 2006, A&A, 452, L23
O'Dea C. P., 1998, PASP, 110, 493
Ohyama Y. et al., 2003, ApJ, 591, L9
Owsianik I., Conway J. E., 1998, A&A, 337, 69
Pei Y. C., 1992, ApJ, 395, 130
Rengelink R. B., Tang Y., de Bruyn A. G., Miley G. K., Bremer M. N., Röttgering H. J. A., Bremer M. A. R., 1997, A&AS, 124, 259
Reuland M. et al., 2003, ApJ, 592, 755
Richards G. T. et al., 2003, AJ, 126, 1131
Richards G. T. et al., 2004, ApJS, 155, 257
Saito T., Shimasaku K., Okamura S., Ouchi M., Akiyama M., Yoshida M., Ueda Y., 2006, ApJ, 648, 54
Schneider D. P. et al., 2003, AJ, 126, 2579
Smith D. J. B., Jarvis M. J., 2007, MNRAS, 378, 49
Smith D. J. B., Jarvis M. J., Lacy M., Martinez-Sansigre A., 2008, MNRAS, Ar XiV e-prints, preprint (arXiv:0806.4384v1)
Steidel C. C., Adelberger K. L., Shapley A. E., Pettini M., Dickinson M., Giavalisco M., 2000, ApJ, 532, 170
Tadhunter C., Marconi A., Axon D., Wills K., Robinson T. G., Jackson N., 2003, MNRAS, 342, 861
Urry C. M., Padovani P., 1995, PASP, 107, 803
Vanden Berk D. E. et al., 2001, AJ, 122, 549
van Ojik R., Röttgering H. J. A., Miley G. K., Hunstead R. W., 1997, A&A, 317, 358
Villar-Martín M., Vernet J., di Serego Alighieri S., Fosbury R., Pentericci L., Cohen M., Goodrich R., Humphrey A., 2002, MNRAS, 336, 436
Webster R. L., Francis P. J., Peterson B. A., Drinkwater M. J., Masci F. J., 1995, Nat, 375, 469
Weidinger M., Møller P., Fynbo J. P. U., Thomsen B., 2005, A&A, 436, 825
Whiting M. T., Webster R. L., Francis P. J., 2001, MNRAS, 323, 718
Willott C. J., Rawlings S., Jarvis M. J., Blundell K. M., 2003, MNRAS, 339, 173
Wilman R. J., Jarvis M. J., Röttgering H. J. A., Binette L., 2004, MNRAS, 351, 1109
Wilman R. J., Gerssen J., Bower R. G., Morris S. L., Bacon R., de Zeeuw P. T., Davies R. L., 2005, Nat, 436, 227

This paper has been typeset from a TEX/LATEX file prepared by the author.